Rare Metal Materials and Engineering
Volume
Available online at **www.rmme.ac.cn**

Science Press

Cite this article as: Rare Metal Materials and Engineering,

ARTICLE

https://doi.org/10.12442/j.issn.1002-185X.20240563

Study on erosion resistance and damage evolution of Ti-doped Ta_2O_5 high transmittance coatings

Ye Borui[1], Chao Rui[2, 3]

[1] School of Mechanical Engineering, Hefei University of Technology, Hefei 230009, China; [2] School of Mechatronics Engineering, Henan University of Science and Technology, Luoyang, 471003, China; [3] Henan Key Laboratory for Machinery Design and Transmission System, Luoyang, 471003, China;

Abstract: In order to verify the wear resistance and erosion resistance of Ti-doped Ta_2O_5 coating (TTO), a series of TTO coatings were prepared by magnetron sputtering technology by controlling the power of Ti target. The growth structure, microstructure and tribological properties of TTO coatings with Ti target power were studied. After the erosion test, the variation of erosion damage behavior of TTO coatings with mechanical properties under different erosion conditions was further studied. The results show that the TTO coatings eliminates the roughness, voids and defects in the material due to the mobility of the adsorbed atoms during the growth process, and a flat and dense smooth surface is obtained. Tribological tests show that the TTO coatings is mainly characterized by plastic deformation and micro-crack wear mechanism. Higher Ti target power can improve the wear resistance of TTO coatings. The results of the erosion test show that the impact crater, furrow, micro-cutting, brittle spalling and crack formation are the main wear mechanisms of the TTO coatings samples under erosion.

Key words: Ti-Ta_2O_5 coatings; organizational structure; tribological properties; erosion behavior; damage law

As a clean, sustainable and widely distributed new type of renewable energy, solar energy is the main technology leading energy transformation to mitigate climate change [1-3]. Because photovoltaic power generation is scalable and easy to disperse, its potential is huge [4]. Photovoltaic power generation has increased significantly and has become the main source of electricity in clean energy [5]. Photovoltaic power generation has fundamentally increased the importance of renewable energy [6, 7]. Globally, photovoltaic power generation accounts for 6.3 % and 1.7 % of installed capacity and power generation, respectively [5]. At this stage, the most advanced technology for converting solar radiation into electrical energy is photovoltaic (PV) solar panels and concentrating solar thermal (CSP) systems [8-10].

The desert area is rich in solar energy and rich and poor in land resources, which is the best choice for the construction of large-scale photovoltaic power stations [11]. The latest research on climate change shows that the frequency of dust storms in desert areas has increased significantly. Dust storms can seriously affect the performance of solar energy collection systems, especially photovoltaic systems [12]. The transparent glass cover plate in the photovoltaic power generation system module is the top layer, which is designed to protect the photovoltaic cells from the impact of dust erosion. Debris and sand in desert areas can also cause erosion and wear on the surface of photovoltaic panels under the action of storms. Erosion and wear of the photovoltaic panel surface caused by sand erosion and the cleaning process required to remove deposited particles may result in a decrease in optical transmittance, or even permanent loss [13-15]. The damage caused by sand particles on the surface of the glass protective cover depends on the intensity of the dust storm, which is essentially related to the wind speed, the size and shape of the incident particles and the duration of the dust storm [16-18]. The reduction or even failure of photoelectric conversion efficiency is a major problem in the desert environment. The accumula-

Received date:
Foundation item: NSFC(××××)
Corresponding author: Chao Rui, Ph.D., Professor, School of Mechatronics Engineering, Henan University of Science and Technology, Luoyang, 471003, P. R. China, E-mail: chaoruibr@163.com

tion and erosion of dust particles on the surface of photovoltaic modules are the main factors for the overall performance degradation of photovoltaics [19-21]. In order to maintain the efficiency of the system, it is necessary to consider protecting the outer surface of the glass cover plate in the photovoltaic module, which is usually made of transparent glass [14]. Therefore, transparent glass is required to ensure high transparency of the solar panel to solar radiation, while providing the necessary mechanical properties to protect the surface of the photovoltaic system from harsh environments [22].

In order to protect photovoltaic panels from sand erosion damage, the application of high-performance coatings seems to be an irreplaceable choice [23,24]. When eroded by irregular gravel, the coatings should be harder than the erosion agent in addition to having stronger adhesion and denser microstructure to improve the corrosion resistance [25]. There have been many studies on erosion resistance coatings. Naveed M et al. [26] studied the effect of Ti2AlC MAX phase coating annealed in vacuum environment on the high-speed particle erosion resistance of Ti6242 alloy surface. The ability to use the MAX phase coatings as an erosion protection medium for engine components exposed to similar erosion conditions was demonstrated. Dario F et al. [27] discussed the effect of ZrO_2 doping on the microstructure, optical and mechanical properties of multi-layer TiO_2/SiO_2 coatings. The overall goal is to synergistically enhance the optical and mechanical properties of multi-layer coatings. Wiesinger et al. [28] conducted artificial dust storm tests on four different anti-reflection (AR) coatings deposited on borosilicate glass and evaluated their corrosion resistance. Metals usually have good ductility and better resistance to plastic deformation. Ti has been widely used due to its high strength and low elastic modulus. The alloying of Ti and Ta with similar ion size can improve the passivation performance of the coatings [29]. However, the effect of Ti doping on the erosion resistance of T_2O_5 coatings has not been studied. In order to prepare TTO coatings with excellent erosion resistance, it is necessary to study the effects of different Ti contents on the microstructure and erosion resistance of T_2O_5 coatings.

In this paper, TTO high transmittance coating was prepared by magnetron sputtering technology doped with Ti element. The microstructure, mechanical and tribological properties of TTO coatings were studied. The erosion wear resistance of TTO coatings was studied by a self-designed fully enclosed micro-particle erosion tester. In addition, the erosion resistance and erosion damage evolution process of TTO coatings was analyzed by changing the wind speed, particle flow rate and erosion angle. Finally, the erosion wear mechanism of TTO coatings under different erosion conditions was revealed by scanning electron microscope (SEM) and energy dispersive spectrometer (EDS). The study of the mechanical and erosion resistance properties of the TTO coatings enables us to predict the durability and efficiency of the glass cover applied to solar panels as a protective coatings.

1 Experiment

1.1 Deposition of TTO coatings

The films were deposited using RF-DC magnetron co-sputtering with Ta_2O_5 and Ti targets with a size of Ø50×3 mm and 99.9% purity by JGP045CA RF sputtering system. The back-bottom vacuum was pumped to below 5×10^{-4} Pa, the deposition pressure was 0.8 Pa, and a target-substrate distance of 120 mm. Because the photovoltaic power generation system component is a transparent glass as a protective cover, the high-transparent glass is also selected as the substrate during the experiment. The substrates are highly transparent quartz glasses and silicon substrates (Si 100). Si wafer is selected as the substrate in order to obtain the coating cross section more conveniently and analyze the microstructure. The substrates were ultrasonically cleaned with acetone, anhydrous ethanol, and deionized water for 10 min with SCIENTZ-450 (Xinzhi Freeze-drying Equipment Co., Ltd.) equipment before deposition, dried with compressed air, and prepared for use. Pre-sputtering by glow discharge for 10 min to obtain a clean target surface before deposition of the film and the substrates were supported on a rotational (10 rpm) base. The Ti-Ta_2O_5 thin films were deposited at different sputtering power. Table 1 is the preparation parameters of the coatings.

Table 1 Deposition parameters of the TTO coatings

Samples	Target power (W)		Flow of Ar (sccm)	Deposition pressure (Pa)
	Ti (DC)	Ta_2O_5 (RF)		
S1	30	120	40	0.8
S2	40	120		
S3	50	120		
S4	60	120		

1.2 Sand erosion experiment

Analyze the actual installation environment of photovoltaic panels. According to ASTM-G76 standard [16, 25], the erosion resistance of TTO coatings in wind-sand environment was simulated. Through the self-designed fully enclosed micro particle erosion testing machine. The wind speed range of the device is 0~25 m/s. The sample scaffold can be freely adjusted from 0º~90º. Particle flow is controllable. The erosion test principle is shown in Fig. 1 (a). The erosion test uses quartz sand with a particle size range of 80-160μm. The shape of quartz sand is extremely irregular, with sharp edges and corners, as shown in Fig.1 (b). All tests are carried out at room temperature. Before and after the test, the samples need to be ultrasonically cleaned for five minutes to remove the residual gravel. The coatings samples S1 and S2 showed high light transmittance. Among them, the transmittance of the coatings samples S1 and S2 in the wavelength range of 220 nm ~ 850 nm fluctuates in the range of

72 % ~ 88 %. The maximum transmittance of the coatings samples S1 and S2 was ~ 93.31 % and 90.93 %, respectively. The reflectivity of the coatings samples S1 and S2 in the wavelength range of 220nm-850nm is less than 25 %. The band gaps of S1 and S2 are 3.98 eV and 3.76 eV, respectively. We have done the corresponding research in the literature [21]. Therefore, this paper mainly studies the erosion test of S1 and S2 coating samples. The specific particle erosion test parameters of TTO coatings is shown in Table 2.

Table 2 TTO coatings erosion test parameters

Samples	Wind speed(m/s)	Angle(°)	Granular flux(g/s)	Time(s)
S1、S2	15	90	0.75	
S1、S2	15	30	0.75	60
S1、S2	15	90	1	

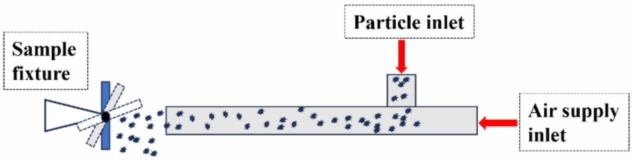

(a) Erosion test principle

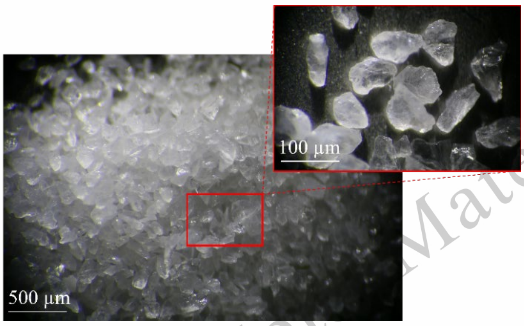

(b) Erosion particle morphology

Fig. 1 Erosion test principle and erosion particles of the TTO coatings

1.3 Morphology characterization of the coatings before and after erosion

Microstructure and surface structure of TTO coatings before and after erosion test. The nanostructure of TTO coatings was obtained by high resolution transmission electron microscopy (TEM, JEM-F200(URP)) at an accelerated voltage of 200 kV. The state of TTO coatings before and after erosion test was characterized by scanning electron microscope (SEM, Zeiss Sigma 300), energy dispersive spectrometer (Smart EDS) and atomic force microscope (AFM, Bruker Dimension Icon). The nanoindentation (ZDT075-075) was used to apply a load of 25 mN, and the indentation depth was not more than 10% of the film thickness, and the microhardness (H) and elastic modulus (E) of the film were obtained. The material high-frequency linear super-smooth testing machine (RTEC MFT-5000) was used. The GCr15 steel ball with a diameter of 5 mm was used. The load of the reciprocating friction test was 0.5 N, the reciprocating distance was 6 mm, the frequency was 20 Hz/s, and the test temperature was room temperature. The failure mechanism and wear traces of the TTO coatings was characterized by SEM.

2 Results and Discussion

2.1 Surface and cross-sectional morphology

Fig.2 shows the cross-sectional morphology and surface morphology of the TTO coatings. The cross-sectional morphology of the TTO coatings shows that the coating is grown in a single layer structure, and the TTO coatings is uniformly bonded to the surface of the substrate. The TTO coatings shows a very obvious columnar structure growth during the growth process. Observing the cross-section morphology of the S1 coatings sample in Fig.2 (a), it was found that a few microcracks appeared. However, with the increase of Ti target power, the cross-section morphology of S2-S4 coatings samples shows that the columnar structure is more closely packed, as shown in Fig. 2 (c-d) cross-section morphology. The occurrence of such phenomena is related to the diffusion energy of atoms. Studies have shown that substrate temperature, working pressure, sputtering power and other parameters will affect the diffusion energy during atomic deposition, which in turn affects the microstructure of the coating [30]. In this study of TTO coatings, the input power has a similar effect on the microstructure of the coating. In the deposition process of S1 coatings sample, the lower sputtering power leads to the diffusion energy is not enough to make the sputtering atoms migrate on the substrate surface, which leads to the phenomenon of loose accumulation and micro cracks in the S1 coatings sample. On the contrary, in the S2-S4 coatings samples at higher sputtering power, the sputtering atoms obtain more energy and can quickly diffuse and grow in a columnar structure at the beginning of the deposition. Therefore, we can conclude that all TTO coatings samples have no obvious cracks or only defects, which indicates that the columnar structure is formed in a specific direction [31]. It can also be observed that the thickness of the coatings is uniform. The thicknesses of TTO coatings S1, S2, S3 and S4 samples were measured to be 405.3 nm, 403.1 nm, 407.1 nm and 401.7 nm, respectively. The surface of the TTO coatings is smooth and dense, and there are no micro-cracks and large-area voids. Due to the bombardment of high-energy particles, the mobility of adsorbed atoms during the growth of TTO coatings is improved, and the roughness, voids and defects in the material are eliminated, thereby obtaining a smoother coatings surface [32,33].

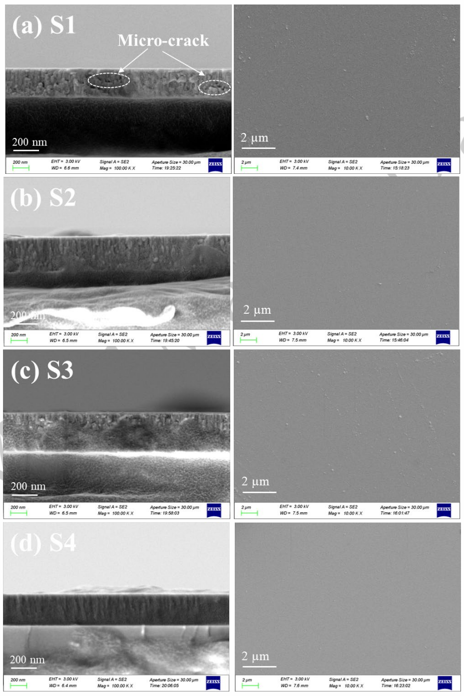

Fig. 2 Surface and cross-section morphology of TTO coatings

Fig. 3 shows the typical TEM image of TTO coatings. The overall crystallinity and morphology of the TTO coatings were evaluated according to the TEM microscopic images. Analysis of Fig. 3 (a) shows that the TTO coatings is stacked by layered structures during the deposition process. Analysis of Fig.3 (b) and (c) high-resolution constituency map and electron diffraction map of the selected area. Fig.3 (c) diffraction pattern does not appear clear lattice fringes, indicating that the phase structure of TTO coatings is mainly amorphous phase.

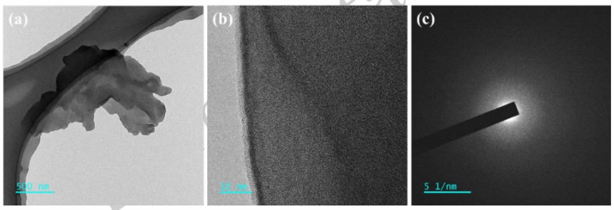

Fig. 3 TEM diffraction pattern of TTO coatings

2.2 Tribological properties

The friction and wear behaviors of TTO coatings samples on glass substrates were compared using a high-frequency linear super-slip tester. The SEM morphology of TTO coatings samples S1-S4 after tribological test is shown in Fig.4. The wear track width of the TTO coatings sample was measured at least four locations. The wear track width of the TTO coatings sample S1-S4 is about 106.1 ± 3nm. The TTO coatings samples S1-S4 have broken and cracks along the edge of the wear track, as shown in Fig.4 (a-d). In order to study the wear behavior of TTO coatings in detail, the wear track was analyzed by SEM, and the element mapping and quantitative analysis of the composition of S1 coating sample were carried out by EDS, as shown in Fig. 4 (a, I, II), (b, I, II), (c, I, II), (d, I, II) and (e, f, g, h). The wear track of S1-S4 coating samples shows that the surface of TTO coatings after friction and wear test is seriously damaged.

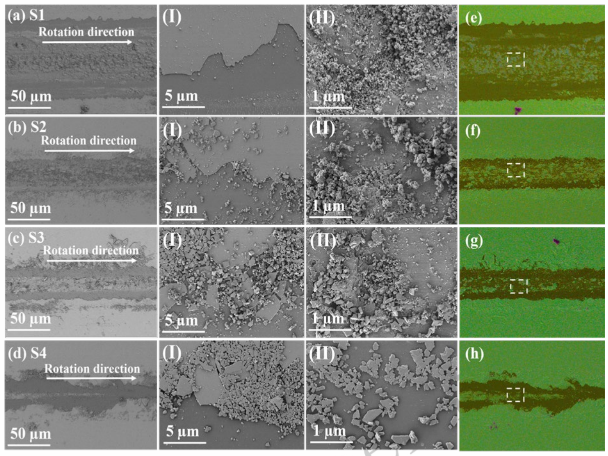

Fig. 4 Friction and wear and wear trace morphology of TTO coatings

Fig.4 (a, I, II) and (b, I, II) show that spalling and partial cracks appear in the friction contact area of TTO coatings samples S1 and S2. The spalling morphology is mainly granular structure, and some smaller particle debris particles are compacted to form a protective coating in the wear area. The friction layer is formed by material transfer and wear traces and cracks that pass through all layers [34]. Fig.4 (c, I, II) and (d, I, II) show that the spalling area of the friction contact area of the TTO coatings samples S3 and S4 increases. The spalling morphology is mainly characterized by a mixed structure of small fragments and fine particles. The TTO coatings samples S3 and S4 have higher cohesion, thus improving the surface plasticity. The friction layer observed by is formed by debris generated during sliding contact tests, which presses the wear area through reciprocating motion [35]. The TTO coatings is mainly characterized by plastic deformation and micro-crack wear mechanism. Further analysis of Fig.4 (e-h) shows that the content of Ta and Ti atoms in the selected area of S1 and S2 friction layers of TTO coatings samples is higher than that of S3 and S4. Therefore, it is considered that the TTO coatings samples S1 and S2 have stronger wear resistance.

2.3 Erosion performance and mechanism analysis

According to the erosion test parameters in Table 2, the simulated particle erosion test of TTO coatings was carried out. Fig.5 (a, b, c) and Fig.5 (c, d, e) are the erosion area damage domain diagrams of the surface of the TTO coatings S1 and S2 samples after the erosion test. Compared with the surface morphology of TTO coating in Fig.2, it was found that the surface of S1 and S2 coating samples was smooth and flat before erosion test. After the erosion test, the surface of the TTO coatings was broken, and the number of cracks and pits gradually increased with the extension of the erosion time. The plastic deformation of the surface morphology of the S1 coatings sample is larger and the situation is more complicated. Fig.5 (g) shows that the erosion damage area of TTO coating sample S1 is larger than that of TTO coatings sample S2 under the same erosion parameters. It may be related to the hardness and elastic modulus of the coatings. H/E and H3/E2 are parameters reflecting the ability of materials to resist plastic deformation, which are usually used to evaluate the toughness and wear resistance of materials [36,37]. The variation of H/E and H3/E2 of TTO coatings samples S1 and S2 is shown in Fig. 6. The H/E and H3/E2 values of the S2 coatings samples were higher than those of the S1 coatings [21]. High hardness, toughness and resistance to plastic deformation can reduce the peak impact force and energy absorption of the coatings during erosion [38].

We analyzed the micro-morphology of TTO coatings material surface after erosion. The purpose is to study the variation of erosion resistance of TTO coatings under different erosion parameters. Fig.7 is the surface erosion morphology of TTO coatings after different erosion parameters test. The erosion morphology of the TTO coatings shows that a large number of impact pits can be observed in the damaged area of the coatings. These erosion craters are caused by the continuous impact of sharp particles [38]. Due to the low toughness of the TTO coatings, it cannot resist the high-energy impact of hard-corner particles and exhibits brittle spalling. Different surface erosion morphologies correspond to different damage forms of coatings materials during erosion process. Different damage forms can reflect the erosion wear law of TTO coatings.

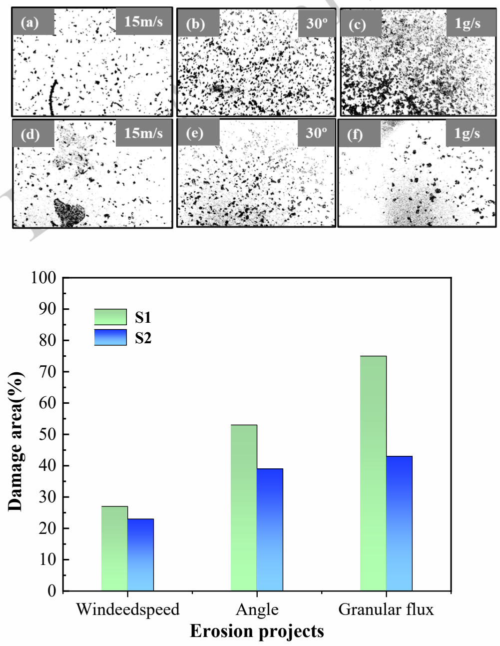

Fig.5 Relationship between surface area damage and erosion parameters of TTO coatings

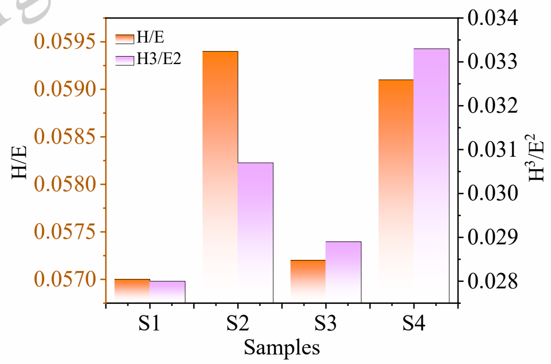

Fig.6 Variation of H/E and H^3/E^2 of TTO coatings samples S1-S4

As shown in Fig.7 (I), the surface of the TTO coatings is dominated by peeling erosion pits at 90º erosion angle. Around the erosion pit is also accompanied by the generation of microcracks, as well as the accumulation of flaking debris and granular structures. Long strip cracks appear around the erosion pit, and these cracks extend. During the continuous impact of the particles, a large area of the TTO coatings was peeled off [39]. The erosion wear forms of TTO coatings is mainly stress fatigue fracture wear and brittle fracture wear.

As shown in Fig. 7 (II), the micro-morphology of TTO coatings after erosion test changed significantly at 30º erosion angle. When the particle erosion angle is low, the damage area of TTO coatings increases. The surface damage form of TTO coatings after erosion test is mainly the cutting and scratching of particles on the coatings.

As shown in Fig. 7 (III), when the particle flow rate is 1g/s, the micro-morphology of TTO coatings after erosion test is more complex and diverse. With the increase of particle flow rate, the impact times of TTO coatings increased significantly. The microstructure after erosion test shows that many cracks and deep erosion pits appear in the erosion area of TTO coatings. Under the micro-cutting action of the corrosive medium, the TTO coatings continuously falls off, forming irregular spalling. Under the action of erosion particles, the spalling debris reattaches to the unpeeled coating [40].

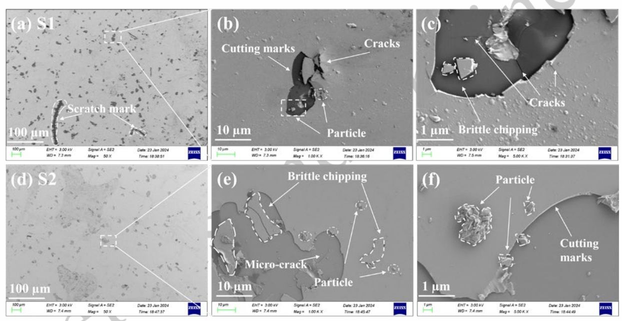

(I) The damage morphology of TTO coatings when the erosion wind speed is 15m/s

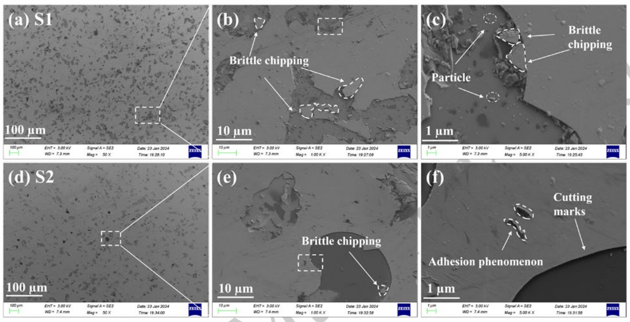

(II) The erosion damage morphology of the TTO coatings at an erosion angle of 30°

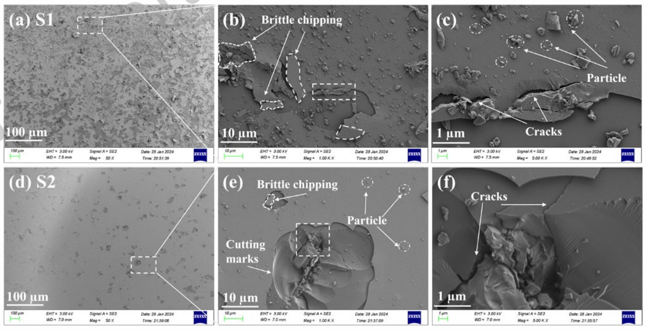

(III) Erosion damage morphology of TTO coatings at particle flow rate of 1g/s

Fig.7 Erosion morphology of TTO coatings under different erosion parameters

Fig.8 shows the distribution of EDS elements on the surface of TTO coatings in some areas after erosion test. It can be seen from the diagram that there is no obvious element aggregation on the surface of TTO coatings after erosion test. The contents of Ti, Ta and O are 4.3%, 74.38% and 21.31%, respectively. The distribution of elements on the erosion surface of TTO coatings plays an important role in revealing the erosion wear mechanism of the coatings, and has certain guiding significance for the design of anti-erosion materials.

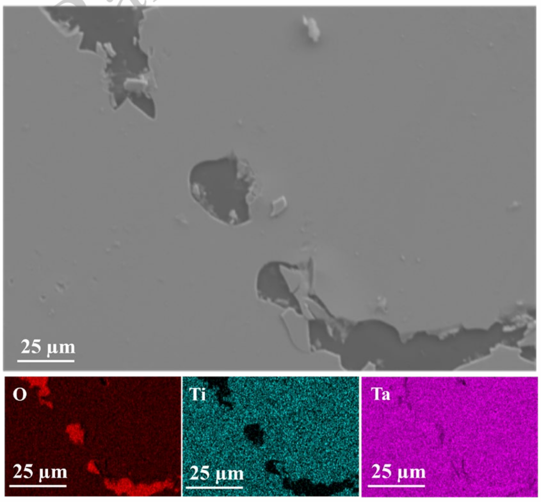

Fig. 8 EDS results of TTO coatings erosion center area

The plasticity index (H^3/E^2) is a parameter to describe the plastic deformation resistance of the coating, and the H^3/E^2 ratio is often used to simply describe the fracture toughness of the solid coatings. Finally, the plasticity indexes of various coatings under different working conditions are listed and analyzed, as shown in Table 3. Cao and Li et al [41, 42] prepared TiN and AlCrN coatings on the surface of titanium alloy according to the problem that aircraft engine blades are vulnerable to sand-dust erosion damage, and evaluated the sand-dust erosion resistance of the samples on the erosion test platform. It is found that TiN and AlCrN coatings can improve the particle erosion resistance of titanium alloy substrate. The erosion wear characteristics of the coating surface mainly include micro-cutting marks, large particle plastic deformation and spalling pits. With the erosion test, the coatings has both plastic material erosion wear mechanism and brittle material erosion wear mechanism. Naveed et al. [43] studied the effect of Ti_2AlC MAX phase coating on the erosion resistance of Ti6242 alloy. The heat treatment process of Ti6242 alloy transforms the spherical microstructure into a dual-phase microstructure, resulting in an increase in surface hardness. With the increase of hardness, the improvement of erosion behavior was observed. After comparative analysis, it is found that the erosion behavior can be predicted by estimating the value of H^3/E^2. Improving the plasticity index of the coatings can improve the erosion resistance of the coatings.

Table 3 H/E and H^3/E^2 of different types of erosion-resistant coatings

Samples	H/E	H^3/E^2
Ti-Ta_2O_5	0.0594	0.0307
TiN	0.0592	0.0799
AlCrN	0.0878	0.1790
Ti_2AlC	0.0583	0.0380

3 Conclusions

In this study, Ti-doped Ta_2O_5 coatings were prepared by magnetron sputtering technology by changing the Ti target power. The phase composition, microstructure and tribological properties of TTO coatings was studied, and the erosion resistance of TTO coatings was evaluated by simulated gravel erosion test.

1) By adjusting the microstructure of the TTO coatings, the change of the sputtering power of the Ti target makes the mechanical properties of the TTO coatings different. Finally, it has a key impact on the friction and wear characteristics and erosion resistance of the TTO coatings.

2) With the introduction of Ti element, the wear resistance of single Ta_2O_5 coatings was improved. When the sputtering power of Ti target is 30W and 40W, the TTO coatings exhibits excellent mechanical and tribological properties. After the

simulated particle erosion test, it was found that the TTO coatings sample S2 showed the best erosion resistance.

3) Further analysis of the microstructure of the TTO coatings after the erosion test found that the failure mechanism of the TTO coatings in the erosion environment is that the particle impact force causes a large number of cracks in the coatings and the brittle spalling caused by the cross propagation of the cracks.

References

[1] Chen Haolei, Dong Yiwei, Yang Hongwei, et al. *Rare Metal Materials and Engineering*[J], 2024, 53(01): 281-95.

[2] Yeligeti M, Hu W, Scholz Y, et al. *Environmental Research Letters*[J], 2023, 18(5): 054027.

[3] Jacobson M Z, Delucchi M A. *Energy Policy*[J], 2011, 39(3): 1154-69.

[4] Comello S, Reichelstein S, Sahoo A. *Renewable and Sustainable Energy Reviews*[J], 2018, 92: 744-56.

[5] Hu M, Song X, Bao Z, et al. *Energies*[J], 2022, 15(17): 6408.

[6] Zakeri B, Paulavets K, Barreto-Gomez L, et al. *Energies*[J], 2022, 15(17): 6114.

[7] Farghali M, Osman A I, Mohamed I M A, et al. *Environmental Chemistry Letters* [J], 2023, 21(4): 2003-39.

[8] Zambrano D F, Villarroel R, Espinoza-González R, et al. *Solar Energy Materials and Solar Cells* [J], 2021, 220: 110841.

[9] Said S A M, Walwil H M. *Solar Energy* [J], 2014, 107: 328-37.

[10] Jiang H, Lu L, Sun K. *Atmospheric Environment* [J], 2011, 45(25): 4299-304.

[11] Xu L Y, Li S Y, Jiang J M, et al. *Solar Energy* [J], 2020, 199: 491-6.

[12] Yilbas B S, Ali H, Khaled M M, et al. *Scientific Reports* [J], 2015, 5(1): 15833.

[13] Pop S C, Abbaraju V, Brophy B, et al. *A Highly Abrasive-Resistant, Long-Lasting Anti-Reflective Coating for PV Module Glass; proceedings of the 40th IEEE Photovoltaic Specialists Conference (PVSC),* Denver, CO, F Jun 08-13, 2014 [C]. 2014.

[14] Humood M, Beheshti A, Meyer J L, et al. *Tribology International* [J], 2016, 102: 237-48.

[15] Zambrano-Mera D F, Espinoza-Gonzalez R, Rosenkranz A, et al. *Solar Energy Materials and Solar Cells* [J], 2023, 250.

[16] Ayadi A, Bouaouadja N, Durán A, et al. *Ceramics International* [J], 2020, 46(8, Part A): 10634-40.

[17] Sansom C, Comley P, King P, et al. *Energy Procedia* [J], 2015, 69: 198-207.

[18] Karim M, Naamane S, Delord C, et al. *Solar Energy* [J], 2015, 118: 520-32.

[19] Beattie N S, Moir R S, Chacko C, et al. *Renewable Energy* [J], 2012, 48: 448-52.

[20] Boyle L, Flinchpaugh H, Hannigan M. *Aerosol Science and Technology* [J], 2016, 50(4): 380-91.

[21] Rui C, Haichao C, Hang L, et al. *Optical Materials* [J], 2024, 147: 114680.

[22] Hegazy A A. *Renewable Energy* [J], 2001, 22(4): 525-40.

[23] Todt J, Pitonak R, Köpf A, et al. *Surface and Coatings Technology* [J], 2014, 258: 1119-27.

[24] Azadi M, Rouhaghdam A S, Ahangarani S, et al. *Surface and Coatings Technology* [J], 2014, 245: 156-66.

[25] Zhang H, Li Z, Ma C, et al. *Ceramics International* [J], 2019, 45(8): 10819-25.

[26]Naveed M, Renteria A F, Nebel D, et al. *Wear* [J], 2015, 342-343: 391-7.

[27] Zambrano-Mera D F, Espinoza-González R, Villarroel R, et al. *Solar Energy Materials and Solar Cells* [J], 2022, 243: 111784.

[28] Wiesinger F, Vicente G S, Fernández-García A, et al. *Solar Energy Materials and Solar Cells* [J], 2018, 179: 10-6.

[29] Chao Rui, Cai Haichao, Li Hang, et al. *Rare Metal Materials and Engineering* [J]., 2024, 53(06):1574-1581

[30] Yang Y H, Chen D J, Wu F B. *Surface and Coatings Technology* [J], 2016, 303: 32-40.

[31] Kaya E, Ulutan M. *Ceramics International* [J], 2022, 48(15): 21305-16.

[32] Zin V, Montagner F, Deambrosis S M, et al. *Materials* [J], 2022, 15(9): 3354.

[33] Kubart T, Gudmundsson J T, Lundin D. 6 - *Reactive high power impulse magnetron sputtering [M]//Lundin D, Minea T, Gudmundsson J T. High Power Impulse Magnetron Sputtering. Elsevier*. 2020: 223-63.

[34] González-Sevilla J E, Berumen J O, Flores-Martínez M, et al. Wear [J], 2022, 498-499: 204337.

[35] Navarro C H, Martínez M F, Carvajal E E C, et al. *The International Journal of Advanced Manufacturing Technology* [J], 2021, 117(5): 1565-73.

[36] Shasha, Y.; Feng, Y.; Minghui, C. W et al. *Met*[J] 2019, 55, 308–316.

[37] Xu S, Xu J, Munroe P, et al. *Scripta Materialia* [J], 2017, 133: 86-91.

[38] Wang S, He W, Zhang H, et al. *Thin Solid Films*[J], 2023, 770: 139757.

[39] Yang Q, Mckellar R. *Tribology International*[J], 2015, 83:

12-20.

[40] Cai X, Gao Y, Cai F, et al. *Applied Surface Science* [J], 2019, 483: 661-9.

[41] Cao Xin, He Weifeng, He Guangyu et al. *China Surface Engineering* [J]. 2016, 29(04): 60-7.

[42] Li Jinjie, Wu Fengfang, Wu Bing. *China Surface Engineering* [J]. 2019, 48(02): 152-8.

[43] Naveed M, Renteria A F, Nebel D, et al. *Wear* [J]. 2015, 342-343: 391-7.

Ti 掺杂 Ta_2O_5 高透光涂层抗冲蚀性能及损伤演变研究

叶博瑞[1]，晁　瑞[2, 3]

(1. 合肥工业大学机械工程学院，安徽　合 230009)

(2. 河南科技大学机电工程学院，河南　洛阳　471000)

(3.河南省机械设计及传动系统重点实验室，河南　洛阳　471000)

摘　要：为了验证 Ti 掺杂 Ta_2O_5 涂层(TTO)的耐磨特性和抗冲蚀性能，采用磁控溅射技术通过控制 Ti 靶功率制备了一系列 TTO 涂层。主要研究了 TTO 涂层随 Ti 靶功率的生长结构、组织形貌、摩擦学特性。进一步研究了冲蚀试验后，TTO 涂层在不同冲蚀条件下，冲蚀损伤行为随力学特性的变化规律。结果表明，TTO 涂层在生长过程中由于吸附原子的迁移率消除了材料中的粗糙度、空隙和缺陷，获得了平整致密的光滑表面。摩擦学试验表明，TTO 涂层主要表现为塑性变形和微裂纹的磨损机制。较高的 Ti 靶功率可以提升 TTO 涂层的耐磨性。冲蚀试验结果表明，冲击坑、犁沟、微切削、脆性剥落和裂纹的形成为 TTO 涂层样品在冲蚀作用下的主要磨损机制。

关键词：Ti-Ta_2O_5涂层；组织结构；摩擦学特性；冲蚀行为；损伤规律

作者简介：晁瑞，男，1995 年生，博士生，河南科技大学机电工程学院，河南　洛阳　471000，E-mail: 215400000002@stu.haust.edu.cn